Proceedings of the 1997 IEEE International
Conference on Control Applications
Hartford, CT • October 5-7, 1997

A Stability Analysis of Controllers subject to Amplitude and Rate Constraints

K. Hui and C.W. Chan

Department of Mechanical Engineering, University of Hong Kong, Pokfulam Road, Hong Kong
khui@hkumea.hku.hk *mechan@hkucc.hku.hk*

keywords: actuator saturation, rate/amplitude constraints, compensators, nonlinear stability

Abstract

This paper investigates the problem of actuators subject to both amplitude and rate constraints. Previous works studied these saturation types separately. Here a compensation structure catering to both constraints is proposed. Realizability of the compensator and its necessary conditions to maintain linear stabilities are presented, conforming to other established results. A simple design method of combining two individually selected compensators is proposed. Discussions focus on analysis of nonlinear stability when both saturations occur simultaneously. The analysis resorts to an approximation of frequency domain methods, enabling necessary conditions for asymptotic stability to be investigated A numerical example demonstrates the procedures and success of the proposed methodology.

1. Introduction

Practical control systems often encounter both rate and amplitude constraints. Because of the complexity associated with multiple nonlinearities, most of the earlier studies considered only amplitude constraints [5,8]. Specific systems with multiple saturations were discussed [1,2,5] but more general results are not available. Nonlinearities in parallel or in series were considered in [1] concerning stability analysis. However, compensated control systems with rate and amplitude constraints are inter-connected and established results could not be applied immediately.

In rate and amplitude constrained systems, the sequence of the type of saturation is important. For example, control valves are often rate constrained first, as it is unlikely that it would immediately reach the fully open (or closed) position giving amplitude constraint. Another example is a robot arm, which is velocity constrained before it reaches its working envelop and becomes position constrained. This realization and identification of the type of saturation sequence has the advantage that compensator designs and stability analysis are simplified.

The content of the paper is as follows. In §2, a compensator is proposed and the stability of the compensated system is studied in §3. A simple compensator design procedure is presented in §4. Stability analysis for the rate and amplitude constrained system with saturation compensation is illustrated via an example in §5.

2. Compensation of rate-amplitude constraints

The general linear system with its actuator subject to both rate and amplitude constraints is shown in Fig.1. Let G be the transfer function of the plant, and the linear controller be described by

$$v = \frac{T}{R} w - \frac{S}{R} y \qquad (2.1)$$

where y is the system output, w is the reference input and v is the controller output. R, S, T are polynomials in Laplace transform variable s for analogue systems or backward shift operator z^{-1} for digital ones. The arguments are omitted for convenience. R is assumed to be monic.

Let the rate and amplitude constraints for the actuator be given by

$$u(t) = \begin{cases} u_{\max}, & v \geq u_{\max} \\ v, & u_{\min} \leq v \leq u_{\max} \\ u_{\min}, & v \leq u_{\min} \end{cases} \qquad (2.2)$$

$$\dot{u}(t) = \frac{du(t)}{dt} = \begin{cases} \dot{u}_{\max}, & \dot{v} \geq \dot{u}_{\max} \\ \dot{v}, & \dot{u}_{\min} \leq \dot{v} \leq \dot{u}_{\max} \\ \dot{u}_{\min}, & \dot{v} \leq \dot{u}_{\min} \end{cases} \qquad (2.3)$$

where $\{u_{\max}, u_{\min}\}$ are the amplitude limits and $\{\dot{u}_{\max}, \dot{u}_{\min}\}$ are the rate limits.

Following [3], the control that cannot be implemented by the actuator due to its rate and amplitude constraints is modelled as nonlinear disturbances and are defined as follows

0-7803-3876-6/97 $10.00 © 1997 IEEE

$$\delta_a(t) = \begin{cases} u_{\max} - v, & v \geq u_{\max} \\ 0, & u_{\min} \leq v \leq u_{\max} \\ u_{\min} - v, & v \leq u_{\min} \end{cases} \quad (2.4)$$

$$\delta_r(t) = \begin{cases} \dot{u}_{\max} - \dot{v}, & \dot{v} \geq \dot{u}_{\max} \\ 0, & \dot{u}_{\min} \leq \dot{v} \leq \dot{u}_{\max} \\ \dot{u}_{\min} - \dot{v}, & \dot{v} \leq \dot{u}_{\min} \end{cases} \quad (2.5)$$

As $\{u_{\max}, u_{\min}\}$ and $\{\dot{u}_{\max}, \dot{u}_{\min}\}$ given in (2.2)-(2.5) are uncorrelated, δ_a and δ_r are independent of each other.

For actuators subject to rate and followed by amplitude constraints, a mathematical model is shown in Fig.2 [cf. 7]. The controller output is first rate constrained, followed by an integral action to give amplitude constraints. As for single saturation systems [4], the rate saturation is to be compensated by P_r and the amplitude saturation by P_a independently. The control expressions are derived below.

Let $R_1(s)=R(s)/s$ for analogue systems or $R_1(z^{-1}) = R(z^{-1})/(1-z^{-1})$ for digital ones, then the rate of change Δv [$= dv/dt$] for the controller output (2.1) can be written as

$$\Delta v = \frac{T}{R_1} w - \frac{S}{R_1} y \quad (2.6)$$

and the amplitude of the controller output is simply

$$v(t) = \int \Delta v(t) dt \quad (2.7)$$

Thus, any constraint applied on Δv leads to rate saturation; and that applied on v results in amplitude saturation.

Assuming a digital configuration, the following equations are obtained for the compensated system shown in Fig.2:

$$v_1 = \Delta v + P_r \delta_r \quad (2.8)$$

$$u_1 = v_1 + \delta_r = \Delta v + [1 + P_r]\delta_r \quad (2.9)$$

$$v = \frac{u_1}{1 - z^{-1}} + P_a \delta_a \quad (2.10)$$

$$u = v + \delta_a = \frac{u_1}{1 - z^{-1}} + [1 + P_a]\delta_a \quad (2.11)$$

Simplification of (2.8)-(2.11) gives

$$v = \frac{T}{R} w - \frac{S}{R} y + \frac{1 + P_r}{1 - z^{-1}} \delta_r + P_a \delta_a \quad (2.12)$$

$$u = \frac{T}{R} w - \frac{S}{R} y + \frac{1 + P_r}{1 - z^{-1}} \delta_r + [1 + P_a]\delta_a \quad (2.13)$$

That is, the linear controller of (2.1) is modified by the saturation disturbances and their compensations as (2.12) and the actuator output becomes that of (2.13).

Using (2.12)-(2.13) and $y=Gu$, the closed-loop system output after simplification is given by

$$y = \frac{G\,T}{R + GS} w + \frac{GR_1(1 + P_r)}{R + GS} \delta_r + \frac{GR(1 + P_a)}{R + GS} \delta_a \quad (2.14)$$

The first term associated with w in (2.14) is the linear system output. The last two terms are due to the rate and amplitude saturations. If there is no compensation, i.e., P_a=0 or P_r=0, the closed-loop system is still affected by actuator saturation.

Under the premise that the linear system is asymptotically stable, and a robustness requirement that it remains asymptotically stable for minor nonlinearities, the compensated output also has to satisfy this condition. Therefore the two compensation terms in (2.14) must be linearly stable and without steady state offsets. And from analysis of single saturation systems [6], the compensators need to satisfy the following conditions:

(P1) $P_a(z^{-1})$ and $P_r(z^{-1})$ have at least one unit delay respectively; or
$P_a(s)$ and $P_r(s)$ are proper.

(P2) poles of $R(z^{-1})P_a(z^{-1})$ and $R(z^{-1})P_r(z^{-1})$ are inside the unit circle; or
real parts of poles of $R(s)P_a(s)$ and $R(s)P_r(s)$ are strictly negative.

(P1) is the realizability condition, ensuring that the compensators are physically implementable. (P2) is a necessary condition for linear stability [6]: otherwise the saturation disturbance terms involving δ_a and δ_r in the closed-loop output of (2.14) will not be asymptotically stable or without steady state offsets. Investigation of nonlinear stability is further discussed below.

3. Stability analysis of the compensated system

The compensated system of Fig.2 is reconfigured to Fig.3 for stability studies. Simple block reductions or algebraic manipulations can both be used to obtain the linear blocks of Fig.3 as

$$G_1 = \frac{1/R_2}{1 + P_a}, \quad G_2 = \frac{GS/R_1}{1 + P_r} \quad (3.1a)$$

$$G_3 = \frac{P_a}{1 + P_a}, \quad G_4 = \frac{P_r}{1 + P_r} \quad (3.1b)$$

$$F_r = \frac{T/R_1}{1 + P_r}, \quad R = R_1 R_2 \quad (3.1c)$$

with $R_2(s) = s$ or $R_2(z^{-1}) = 1 - z^{-1}$ (3.2)

In addition to (P1) and (P2), a necessary condition for the compensation system to be globally stable [6] is

(P3) zeros of $[1+P_a(z^{-1})]$ and $[1+P_r(z^{-1})]$ are inside the unit circle; or
real parts of zeros of $[1+P_a(s)]$ and $[1+P_r(s)]$ are strictly negative.

This is because roots of $(1+P_a)$ and $(1+P_r)$ are actually poles of the linear blocks (3.1), which must be asymptotically stable in order to guarantee global asymptotic stability [1]. Study of the nonlinear stability is carried out by an approximation using Nyquist plots as follows.

Let $G_C=GS/R$ and assume the nonlinear elements of Fig.3 be replaced by dynamic gains $\{k_a,k_r\}$: k_a for amplitude constraint and k_r for rate constraint. If the system is unconstrained, then $k_a=k_r=1$. The following equations are immediately obtained from Fig.3:

$$u_1 = k_r [F_r w - G_2 u + G_4 u_1] \qquad (3.3)$$

As $w\equiv 0$ in stability analysis, giving

$$u_1 = -\frac{k_r G_2}{1 - k_r G_4} u \qquad (3.4)$$

and $$v = G_1 u_1 + G_3 u = -\left[\frac{k_r G_1 G_2}{1 - k_r G_4} - G_3 \right] u \qquad (3.5)$$

With the dynamic gain assumption, $u = k_a v$ (3.6)

thus $$1 + k_a \left[\frac{k_r G_1 G_2}{1 - k_r G_4} - G_3 \right] = 0 \qquad (3.7)$$

which can be simplified as

$$1 + k_a G_{Ea} = 0 \qquad (3.8)$$

where the equivalent system G_{Ea} for the amplitude constrained system is given by

$$G_{Ea} = \frac{1}{1+P_a} \left[\frac{k_r G_C}{1+(1-k_r) P_r} - P_a \right] \qquad (3.9)$$

Similarly, let G_{Er} be the equivalent system for the rate constrained system, then

$$u = k_a [G_1 u_1 + G_3 u] = \frac{k_a G_1}{1 - k_a G_3} u_1 \qquad (3.10)$$

thus $$v_1 = -G_2 u + G_4 u_1 = -\left[\frac{k_a G_1 G_2}{1 - k_a G_3} - G_4 \right] u_1 \qquad (3.11)$$

From the dynamic gain assumption, $u_1 = k_r v_1$ (3.12)

giving $$1 + k_r \left[\frac{k_a G_1 G_2}{1 - k_a G_3} - G_4 \right] = 0 \qquad (3.13)$$

which can be simplified as

$$1 + k_r G_{Er} = 0 \qquad (3.14)$$

with $$G_{Er} = \frac{1}{1+P_r} \left[\frac{k_a G_C}{1+(1-k_a) P_a} - P_r \right] \qquad (3.15)$$

Actually, (3.9) and (3.15) can be combined together as

$$[1+(1-k_a)P_a][1+(1-k_r)P_r] + k_a k_r G_C = 0 \qquad (3.16)$$

Both (3.8) and (3.14) are in form of the characteristic equations of some linear systems with proportional controllers. These may thus be viewed as an approximation of the nonlinear system expanded around the operating condition $\{k_a,k_r\}$, and hence be used to study the approximate nonlinear stability of the rate and amplitude constrained system. Clearly, if $k_a = k_r \equiv 1$, (3.16) becomes a linear system.

When using Nyquist plots of (3.9) and (3.15), it is often convenient to consider the systems using $1+G_{Ea}$ and $1+G_{Er}$ instead of (3.9) and (3.15). The Nyquist plots remain the same as the origin of the $1+G_E(j\omega)$-plan corresponds to the $-1+j0$ point on $G_E(j\omega)$-plan. Such a linear translation of the origin is to simplify designs of the compensators [4]. This technique is generalized from single saturation systems previously investigated [6].

A simple graphical method to assess the nonlinear stability of the rate and amplitude constrained system is to plot families of Nyquist curves of (3.9) and (3.15) for $0\le k_a, k_r \le 1$. Circle criteria [1] are then used to check whether the Nyquist curves circumscribe individual circles cutting $[-1/k_a, -1]$ or $[-1/k_r, -1]$ on the -ve x-axis. A further simplification is to check only for crossing-points of Nyquist curves to the left of $-1+j0$ on the -ve x-axis.

With due regard to the fallacy of the Aizermann conjecture [1], indications of cutting points to the left of point $-1+j0$ on the -ve x-axis necessarily infer instability of the rate and amplitude constrained system in certain global regions, although it is *a priori* required to be asymptotically stable locally. Due to the approximation of this analysis, non-existence of cutting points only indicate a likelihood that the rate and amplitude constrained system may be asymptotically stable around the operating condition.

When viewing the Nyquist curve families on the $1+G_E(j\omega)$-plan, the above method of checking cutting-points to the left of the $-1+j0$ point on the $G_E(j\omega)$-plan becomes the inspection of any interception of the Nyquist plots with the entire -ve x-axis. An example is presented in §5 illustrating the procedures.

4. Compensator designs

Given the complicity of rate and amplitude constrained systems, simultaneous designs of compensators $\{P_a,P_r\}$ in (2.12)-(2.13) are difficult. On the other hand, systematic methods to design P_a and P_r individually for its type of saturation alone have been developed [3,4] and found highly successful. Therefore, at least as a first step, it is reasonable to adopt the design strategy, in which P_a and P_r are selected separately using the proposed methods in [3,4], ignoring temporarily the other type of saturation; and then use these designs in (2.12)-(2.13) subsequently.

For any given operating condition, if P_a and P_r are individually designed to be the optimal compensator, $\{(P_a,P_r) \mid (\delta_r\equiv 0: P_a=P_{a\ opt})$ and $(\delta_a\equiv 0: P_r=P_{r\ opt})\}$, with respect to some performance index $J_N(P_a,P_r)$, then by the argument of continuity and smoothness of the cost function surface, $J_N(P_{a\ opt},P_{r\ opt})$ shall not be a local maximum and is a possible candidate as *the* optimal compensator. Given the lack of better designs or further fine tunings, the compensator $(P_{a\ opt},P_{r\ opt})$ can be used in (2.12)-(2.13) when both types of saturation occur under the same operating condition. In the least, it acts as the starting point for searching the 'optimal' compensator.

Additionally, the same performance index can be used to evaluate the performance of a compensator pair $\{P_a,P_r\}$ under varying operating conditions $\{k_a,k_r\}$. In that case the cost functions will become $J_N(k_a,k_r)$. A well discussed compensator is the 'conditioning technique' [eg. 2], which for controller (2.1) is described by

$$P(z^{-1}) = \frac{T(z^{-1})}{T(0)}\frac{1}{R(z^{-1})} - 1 \qquad (4.1)$$

Thus, one possible scheme for compensating the controllers is to use (4.1) accordingly for each of the rate and amplitude constraints. Note that the controller seen by each saturation is different, so that R in (4.1) must be replaced by R_I for the rate constraints.

When measuring the severity of saturation, a characteristic number has be defined [3,4]

$$\lambda = [\,u_{abs} - u_{ss}\,] / [\,t_0\, h\,] \qquad (4.2)$$

where $t_0=T(0)$; h is the input step size; u_{abs} is the maximum unconstrained control demand and u_{ss} is the steady state control signal. λ is found very useful in the design of compensators [4]. Physically it signifies the initial portion of control demands which can be afforded by the actuator; and hence can be used to assess the severity of control saturation.

In evaluating compensator designs, a common performance index is the accumulated sum of square errors (ASE)

$$J(P_a,P_r) = \sum_{t=0}^{\infty} [w(t)-y(t)]^2 \qquad (4.3)$$

Let J_0 be the cost for the unconstrained system, then the normalized sum of square errors (NASE) is defined as

$$\text{NASE} = J_N(P_a,P_r) \triangleq J(P_a,P_r)/J_0 - 1 \qquad (4.4)$$

5. Example

An example is presented below, detailing the procedures of the stability analysis discussed in §4. The observed nonlinear stability behaviours are explained by results obtained using the simple method.

For a digital system and PID controller described by

$$G(z^{-1}) = \frac{0.05z^{-1}(1+0.98z^{-1})}{1-1.95z^{-1}+0.96z^{-2}} \qquad (5.1)$$

$$R(z^{-1})=1-z^{-1},\ S(z^{-1})=T(z^{-1})=5[1-0.9z^{-1}]^2 \qquad (5.2)$$

Adopting scheme (4.1), the two compensators are

$$P_a(z^{-1}) = [-0.8\,z^{-1}+0.81\,z^{-2}\,]/[\,1-z^{-1}\,] \qquad (5.3)$$

$$P_r(z^{-1}) = -1.8\,z^{-1}+0.81\,z^{-2} \qquad (5.4)$$

For unit step input, the steady state control signals are $\{\dot{u}_{ss}=0,\ u_{ss}=0.1\}$. To study the performance of compensators (5.3)-(5.4), the actuator limits are varied for $\{\dot{u}_{ss}\pm\lambda_r t_0 h,\ u_{ss}\pm\lambda_a t_0 h \mid 0<\lambda_r,\ \lambda_a\le 1\}$.

The $J_N(\lambda_r,\lambda_a)$-surface are shown in Fig.4 for $[0.23\le\lambda_r\le 1,\ 0<\lambda_a\le 1]$ and Fig.5 for $[0<\lambda_r\le 0.5,\ 0<\lambda_a\le 1]$. The unstable regions were chopped off for presentation. The isolated island of instability $[0.27<\lambda_r<0.33,\ 0.6<\lambda_a\le 1]$ is unexpected in linear analysis, but can be explained by the proposed method for stability studies. Stable regions A and B in these figures are reflected in plots of the Nyquist curve families of G_{Ea} and G_{Er}, according to (3.9) and (3.15).

When rate constraints are not severe $[0.4\le\lambda_r\le 1]$, increase in amplitude constraint raises cost $J_N(\lambda_r,\lambda_a)$ [Fig.4], but it remains asymptotically stable. This is necessarily true because the unconstrained system must be asymptotically stable to be admitted in the first place. For rate constraints in region $0.27<\lambda_r<0.33$, the system is asymptotically stable only if amplitude constraint is severe $[0<\lambda_a<0.6]$; it is unstable when slightly amplitude saturated $[0.6<\lambda_a\le 1]$.

This is reflected in the existence of interceptions of

the -ve x-axis by the Nyquist curves of $G_{Er}(j\omega)$, shown in Fig.6. The equivalent system $G_{Er}(z^{-1})$ does not cut the -ve x-axis if saturation is severe [k_a<0.01977], and hence would be asymptotically stable in the presence of saturation. The cross-over in Fig.6 necessarily means that system is not globally stable for 0.01977<k_a≤1. Region A (along the λ_a-direction) can thus be explained by interpretations of Fig.6.

For fixed rate constraint levels, $G_{Ea}(j\omega)$-plots are shown in Fig.7 and Fig.8. It is seen that when 0.3198≤k_r≤1, the $G_{Ea}(j\omega)$-plots do not intercept the -ve x-axis and local stability is achieved. For 0.845e-3<k_r<0.3198, the $G_{Ea}(j\omega)$-plots circumscribe the critical point -1+j0 in clockwise direction. System is then not even linearly stable. For k_r<0.845e-3, the $G_{Ea}(j\omega)$-plots no longer intercepts the -ve x-axis and system stability is restored. Combining interpretations of Fig.7 and Fig.8, the stability behaviour around the isolated island of instability [0.27<λ_r<0.33, 0.6<λ_a≤1] is thus explained. In these Nyquist plots, significant higher harmonics for small values of dynamic gains complicate matters and the above explanations might not be stretched under extreme conditions.

6. Conclusion

This paper studies practical control systems subject to rate and amplitude constraints. A compensation structure is proposed and the linear control law is modified by saturation compensation terms. The closed-loop output expression is established. Compensator design strategy is reviewed with regard to methodologies developed for single saturation systems. The main contribution is in the proposition of an approximate method for stability analysis, which enables local stability predictions to be obtained via simple procedures using families of Nyquist plots. A numerical example is used to illustrate the feasibility and success of the proposed method for nonlinear stability analysis.

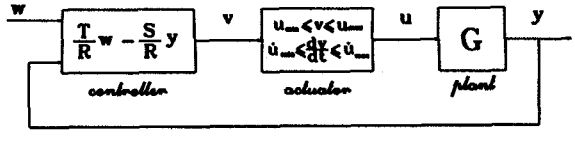

Fig.1 System subject to rate and amplitude constraints

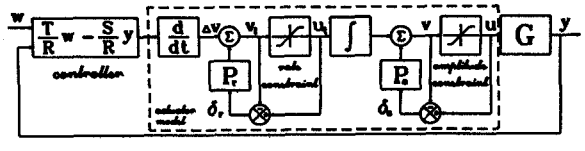

Fig.2 Independent rate and amplitude compensation

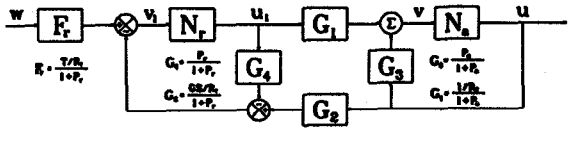

Fig.3 Equivalent system of Fig.2 for stability analysis

References

[1] Atherton, D.P. *Nonlinear Control Engineering*, 1982 Van Nostrand Reinhold

[2] Campo, P.J., Morari, M. and Nett, C.N. *Multivariable Anti-Windup and Bumpless Transfer: A General Theory*, Proc. ACC'89 vol.2 pp.1706-1711 1989

[3] Chan, C.W. and Hui, K. *Design of compensators for actuator saturation*, Proc. IMechE Part I: vol.209 no.3 pp.157-164 1995

[4] Chan, C.W. and Hui, K. *Design of Actuator Saturation Compensators based on Phase Angle Specification*, Preprints 13th IFAC World Congress vol.E pp.155-160 1996

[5] Glattfelder, A.H. and Schaufelberger, W. *Start-up performance of different proportional-integral-anti-wind-up regulators*, Int. J. Control vol.44 no.2 pp.493-505 1986

[6] Hui, K. and Chan, C.W. *Stability analysis of actuator saturation compensation schemes*, Proc. CAI Pacific Symp. '94 pp.45-50 1994

[7] Hui, K. and Chan, C.W. *A Saturation Compensation Approach for Constrained Velocity Algorithms of PID Controllers with Amplitude Limits*, Proc. CAI Symp.97 pp.45-50 1997

[8] Krikelis. N.J. *State feedback integral control with "intelligent" integrators*, Int. J. Control vol.32 no.3 pp.465-473 1980

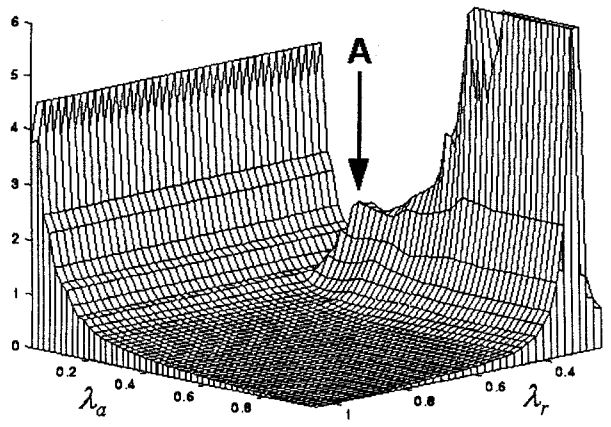

Fig.4 NASE surfaces for $0.23<\lambda_r\leq 1$. Region A is stable [cost function surface truncated at 6].

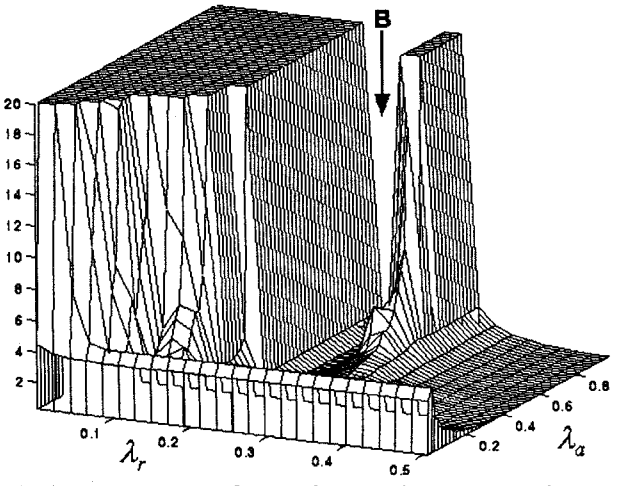

Fig.5 NASE surfaces for $0<\lambda_r\leq 0.5$. Region B is stable [cost function surface truncated at 20].

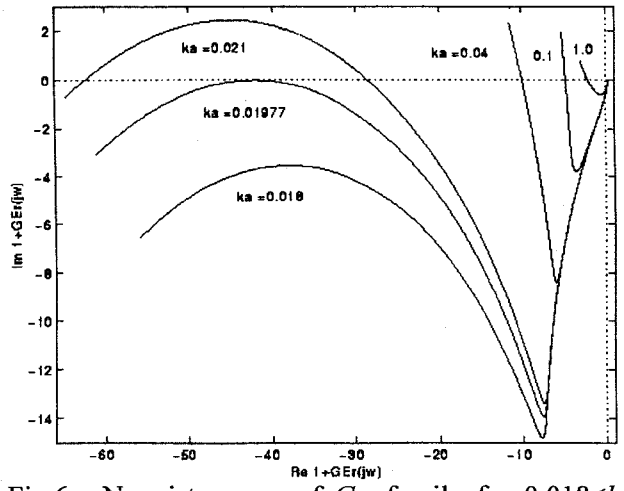

Fig.6 Nyquist curves of G_{Er}-family for $0.018\leq k_a\leq 1$. Cross-over of the -ve x-axis exists for $0.01977\leq k_a\leq 1$.

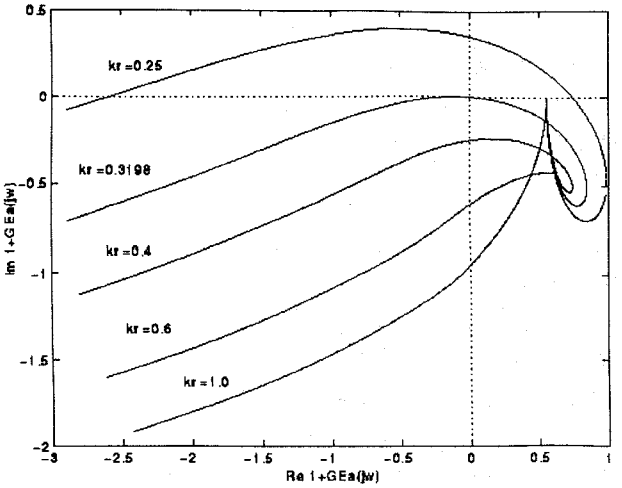

Fig.7 Nyquist curves of G_{Ea}-family for $0.25\leq k_r\leq 1$. Cross-over of the -ve x-axis occurs when $k_r<0.3198$.

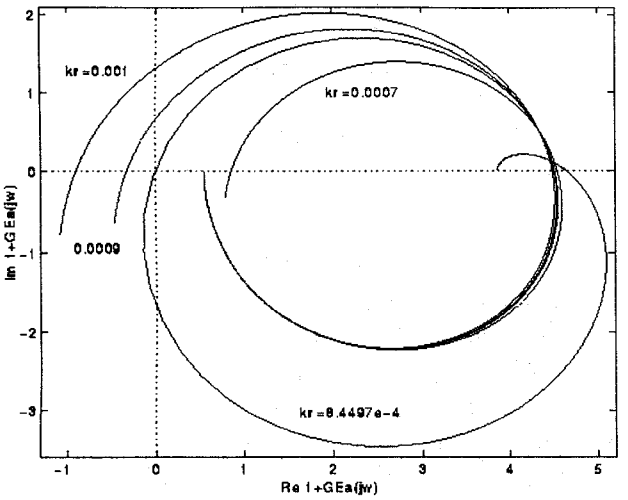

Fig.8 Nyquist curves of G_{Ea}-family for $0.7\text{e-}3\leq k_r\leq 1\text{e-}3$. Cross-over of the -ve x-axis continues until $k_r<0.845\text{e-}3$.